doi:10.1038/nature11740

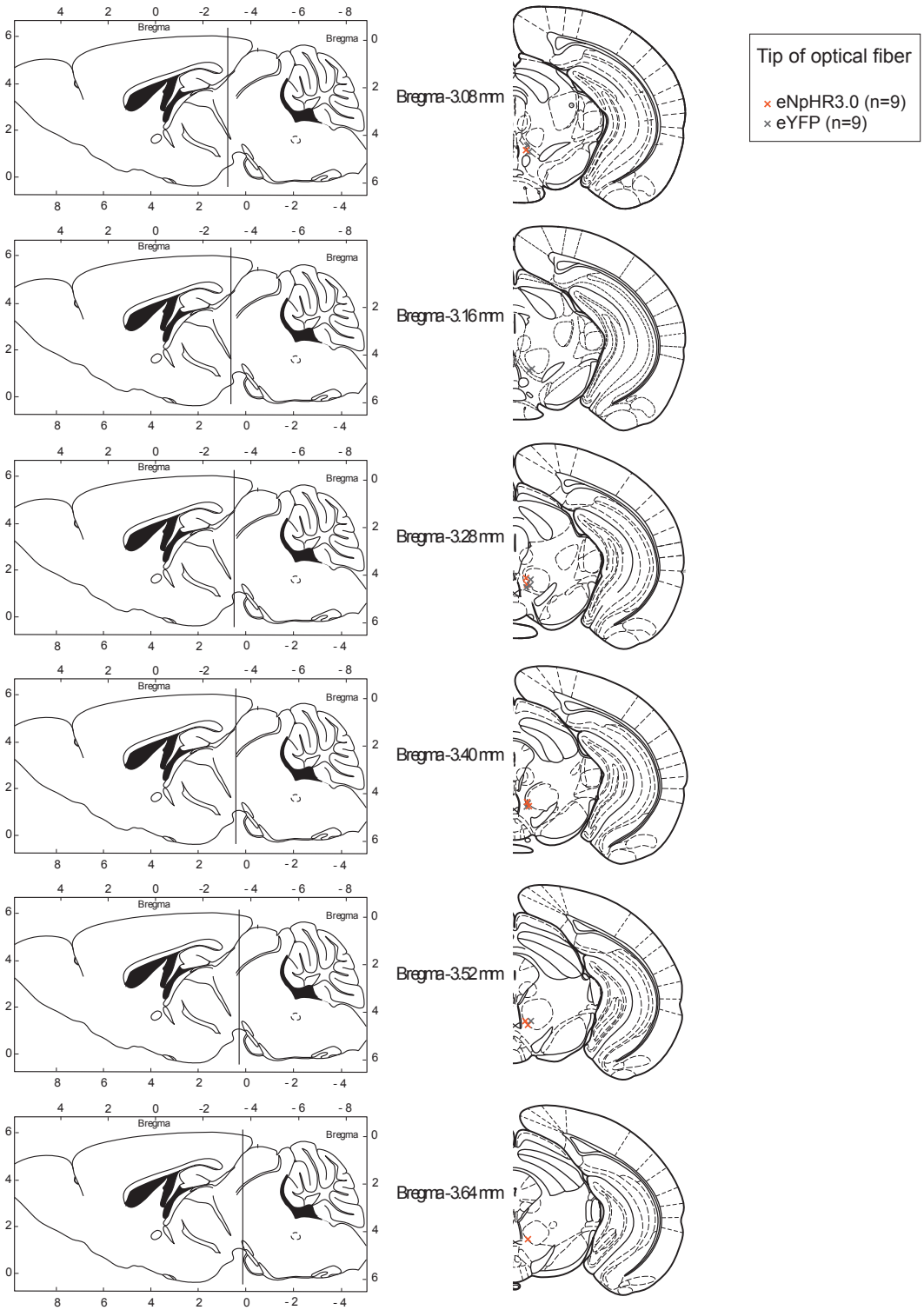

Supplementary Figure 1: Histologically verified placements of the optical fiber for all animals included in Fig. 1 and Supplementary Figure 5a. Expression at the termination of fiber track was also verified (not shown). Symbols for each cohort are shown in the legend (n=9 mice for each group).

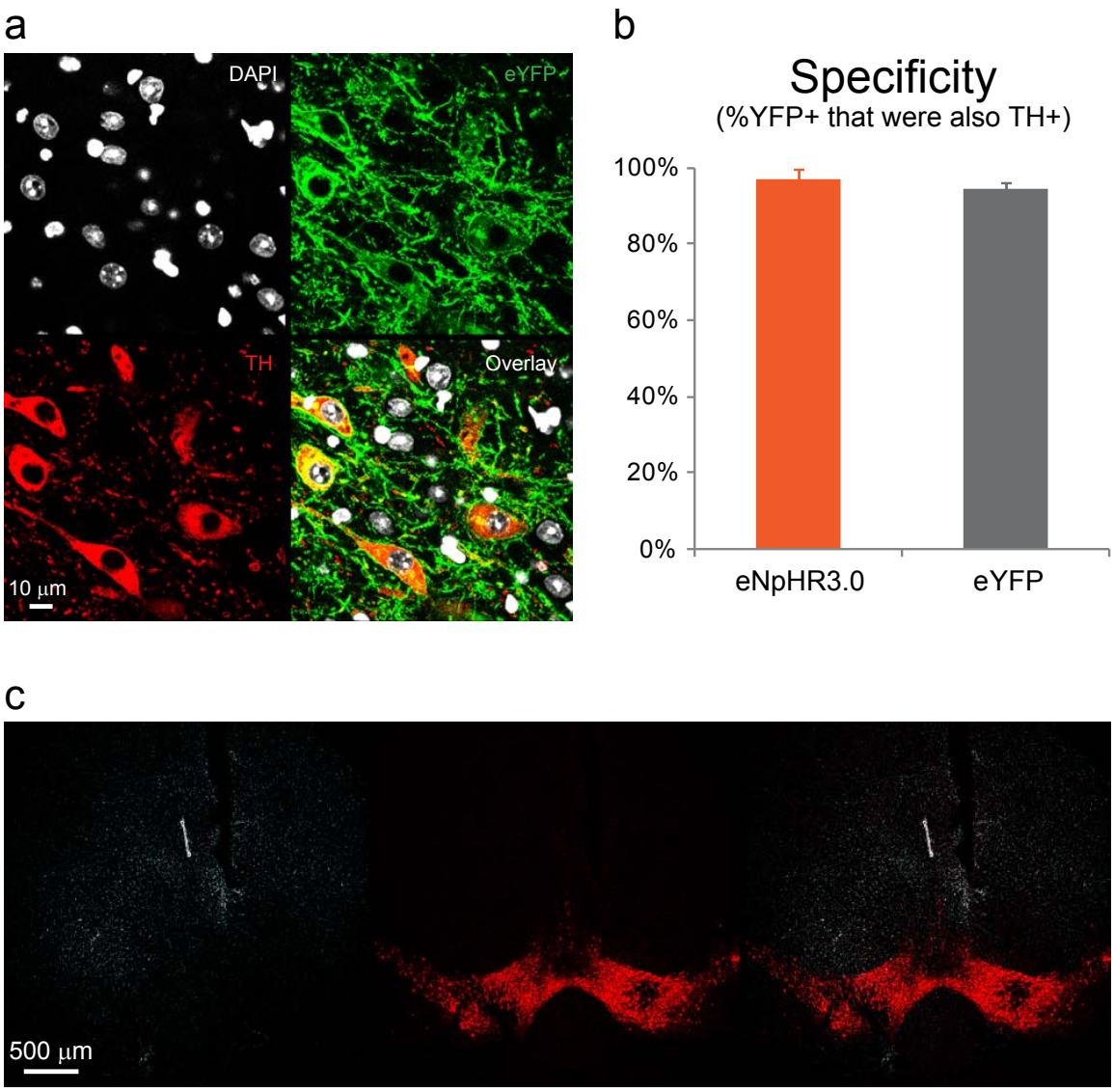

Supplementary Figure 2: eNpHR3.0 is selectively expressed in tyrosine hydroxylase-positive (TH+) neurons. a, Representative high-magnification confocal image of the VTA, showing cells immediately under the optical fiber in a representative eNpHR3.0 animal. b, Animals used in the behavioral experiments described in Figure 1 are included in this population summary of specificity. Cells were counted from z-stacks taken from the region directly below the optical fiber. The mean proportion of eYFP+ neurons that were also TH+ for animals transduced with the Cre-dependent eNpHR3.0-eYFP fusion protein (96.2±3.14%) and for animals transduced with the Cre-dependent eYFP alone (93.3%±2.17%) showed similarly high levels of specificity. c, Low-magnification view showing extent and specificity of transduction.

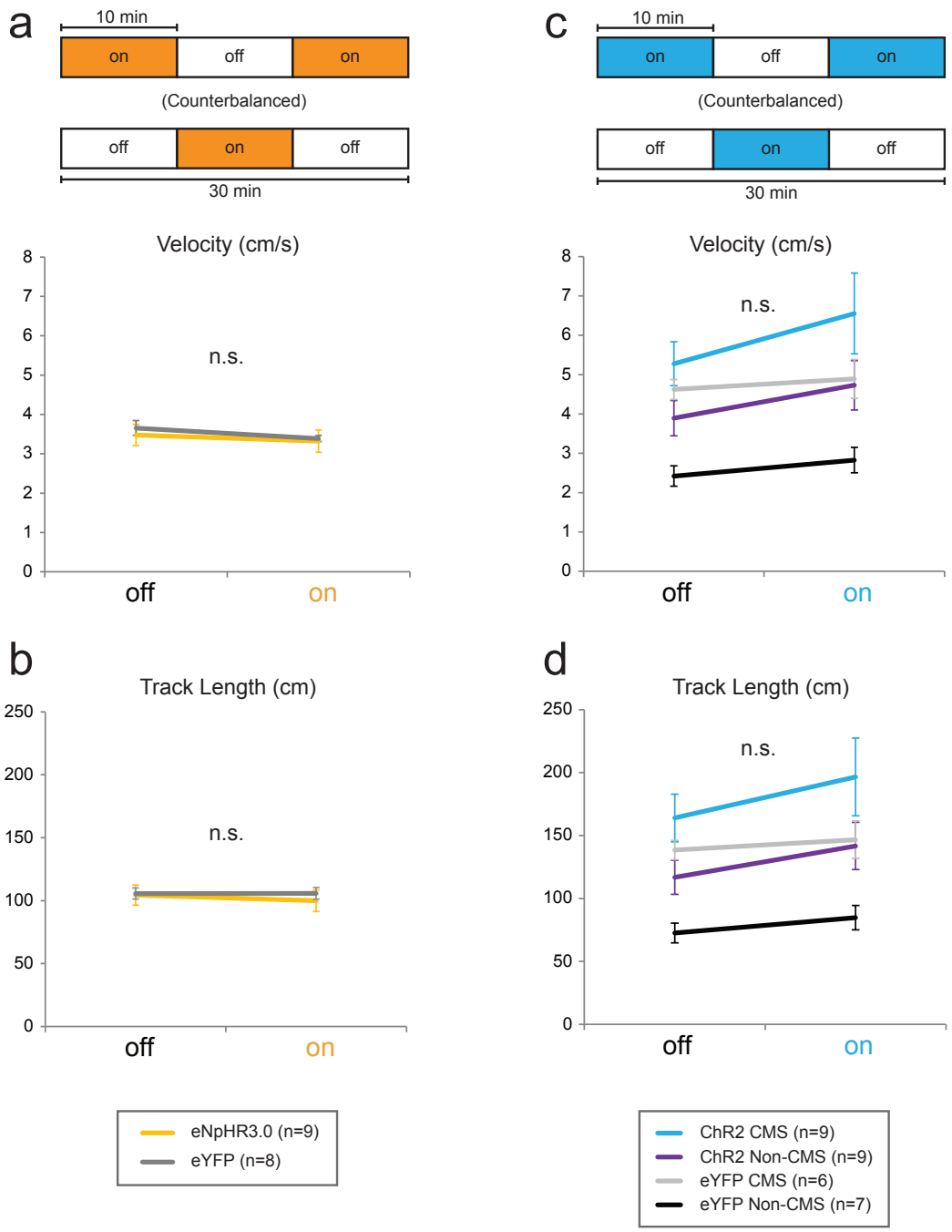

Supplementary Figure 3: Extended open field test session with counterbalanced epoch order. To ensure that the session and epoch durations were long enough to detect significant changes in locomotion, we repeated the open field test with a new cohort of animals. In these tests, we also counterbalanced the order of epochs such that half of the animals in each group were run with each order (ON-OFF-ON or OFF-ON-OFF), using the same illumination parameters (constant illumination for eNpHR3.0 and phasic bursts for ChR2, see methods below). **a**, eNpHR3.0 animals did not show a significant difference from eYFP controls (**a**,**b**). Quantifying locomotion by velocity, using

a repeated measures 2-way ANOVA, we did not observe a significant interaction between light epoch and treatment group ($F_{1,15}$=0.50, *P*=0.4916). **b**, Quantifying locomotor activity by track length, using a repeated measures 2-way ANOVA, we did not observe a significant interaction between light and treatment group ($F_{1,15}$=0.73, *P*=0.4067). **c**, ChR2 CMS and ChR2 non-CMS animals did not show a significant difference from either of the eYFP control groups (**c**,**d**). For velocity, using a 2-way ANOVA, we did not observe a significant interaction ($F_{3,27}$=1.01, *P* = 0.4046). We did, however, observe significant effects of both group ($F_{3,27}$= 5.71, P=0.0037) and light epoch ($F_{1,27}$= 9.26, p = 0.0052). **d**, For track length, using a 2-way ANOVA, we did not observe a significant interaction between light and treatment group ($F_{3,27}$=1.15, *P*=0.3460). We did, however, observe significant effects of both group ($F_{3,27}$= 5.44, P=0.0047) and epoch ($F_{1,27}$= 9.86, P = 0.0041). These group and epoch effects may reflect light-induced changes that extended beyond the light epochs. Given that human patients diagnosed with major depression have shown reductions in gait velocity and stride length[1], such an effect of increased motivation for exploration and/or diminished psychomotor retardation, although subtle, is consistent with reversal of a stress-induced depression-like phenotype.

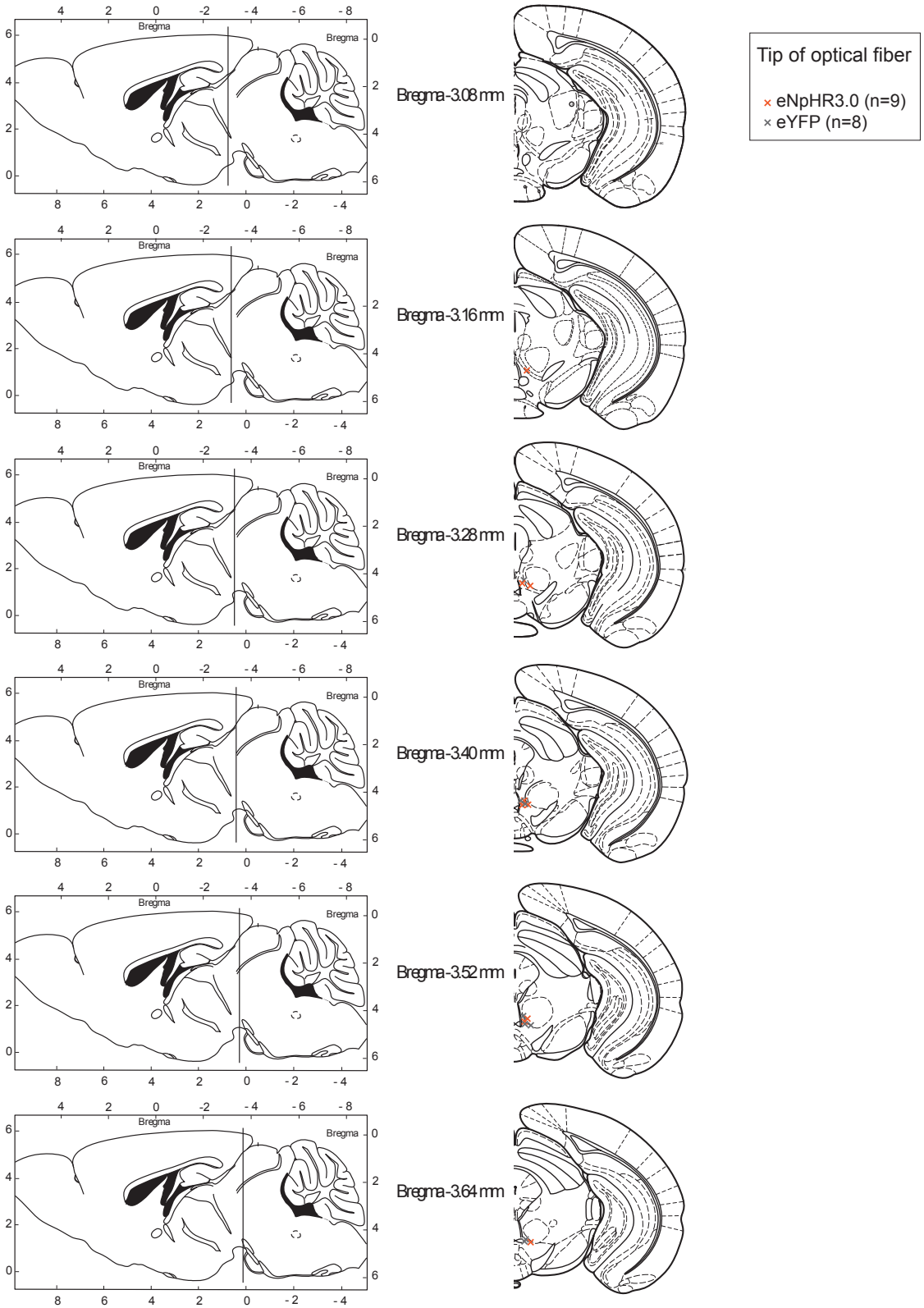

Supplementary Figure 4: Histological verification of fiber tip for all animals in Supplementary Figure 3a and 3b. Crosses indicate the location of all animals confirmed with viral expression in the VTA.

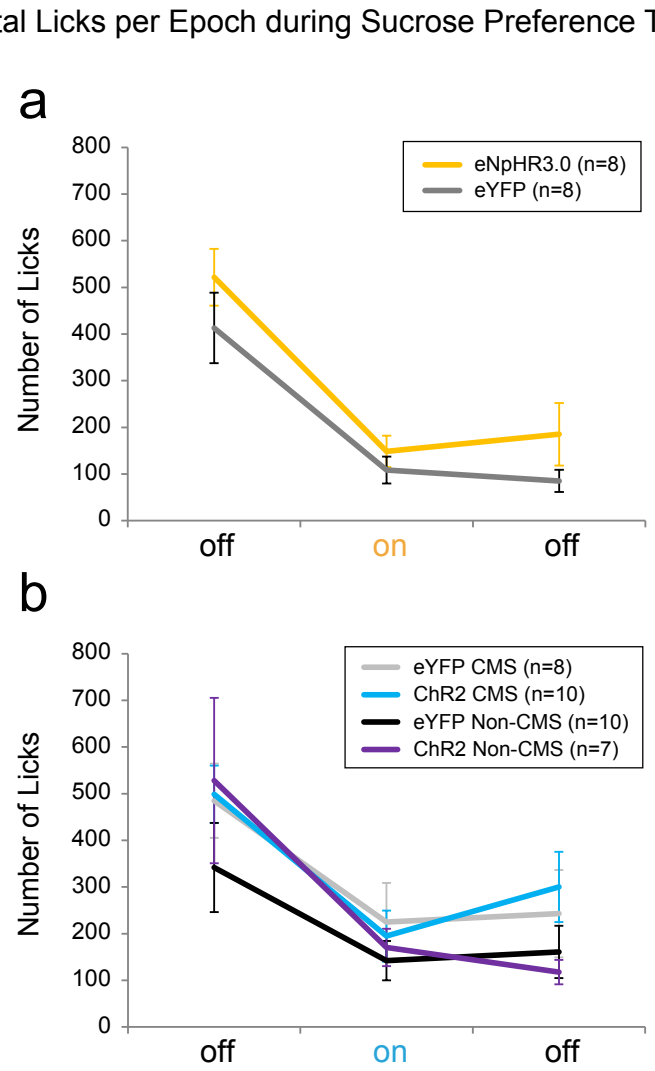

Supplementary Figure 5: Total licks per epoch during sucrose preference test. In addition to the quantification of sucrose preference shown in Fig. 1e and Fig. 2e, we display here the total licks, combining the licking contacts at the water spout and the 1% sucrose spout. All groups showed a similar decrease across the session in licking, likely due to satiety. **a**, For eNpHR3.0 animals and eYFP, on a 2-way ANOVA, we did not observe a significant interaction between group and light ($F_{2,28}$=0.37, p=0.6940). **b**, For ChR2 CMS, ChR2 non-CMS, eYFP CMS and eYFP non-CMS groups, on a 2-way ANOVA, there was no significant interaction between group and light ($F_{6,\ 62}$=1.02, p=0.4239). Thus, changes in sucrose preference were independent of overall consumption.

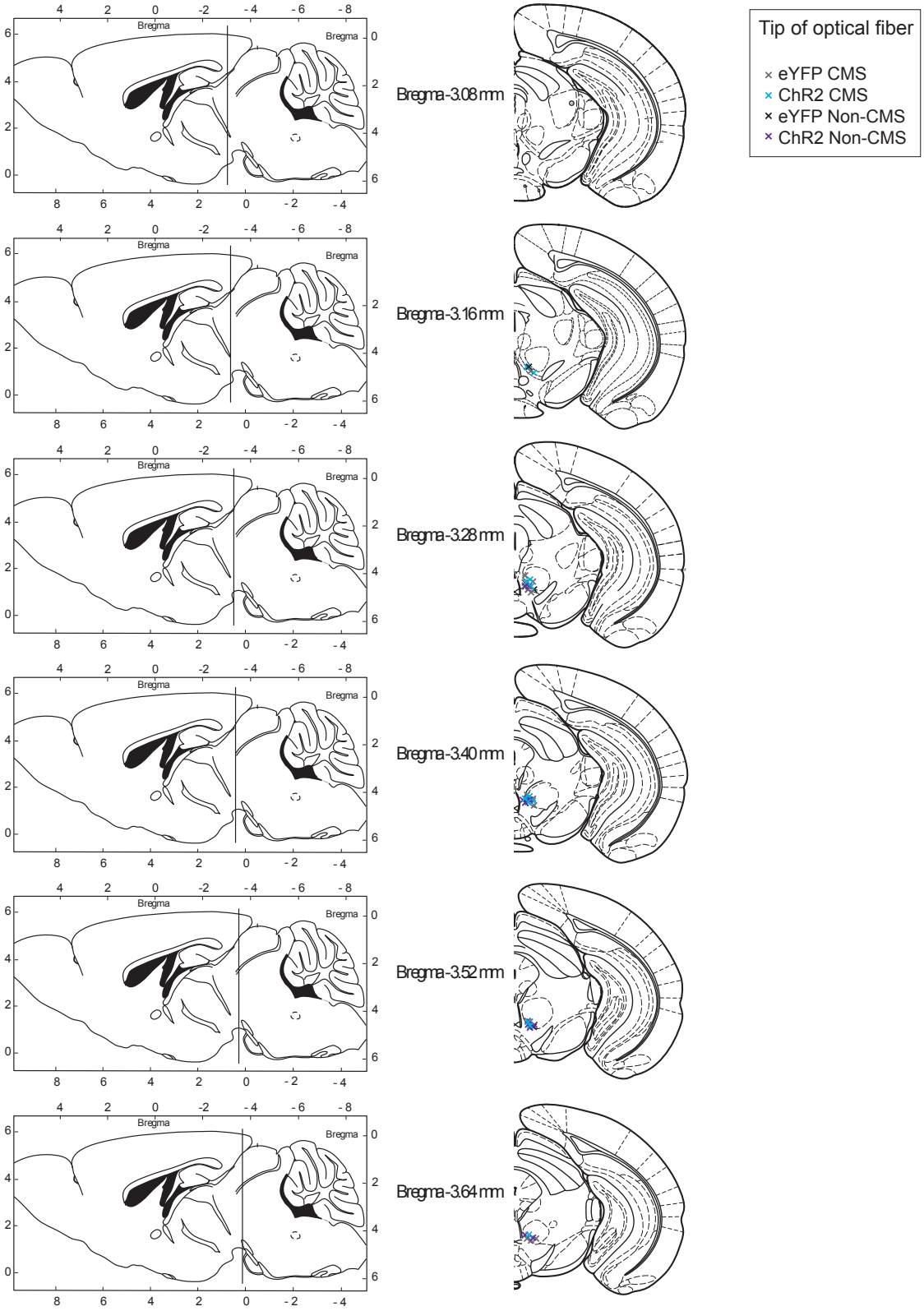

Supplementary Figure 6: Histological verification of fiber tip for all animals included in Fig. 2 and Supplementary Figure 5b. Color of crosses indicates the animal group.

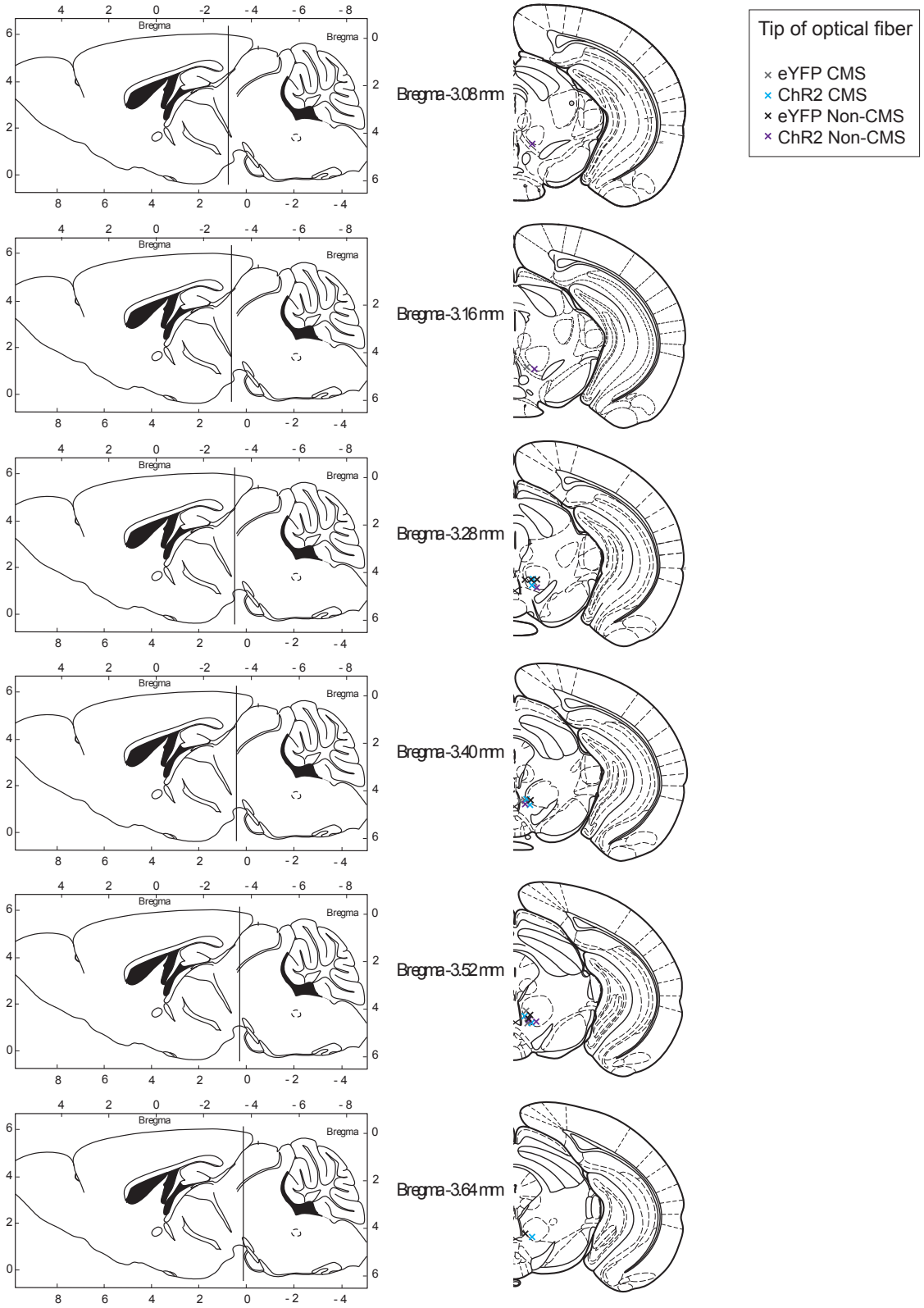

Supplementary Figure 7: Histological verification of fiber tip for all animals in Supplementary Figure 3c and 3d. Crosses indicate the location of all animals confirmed with viral expression in the VTA.

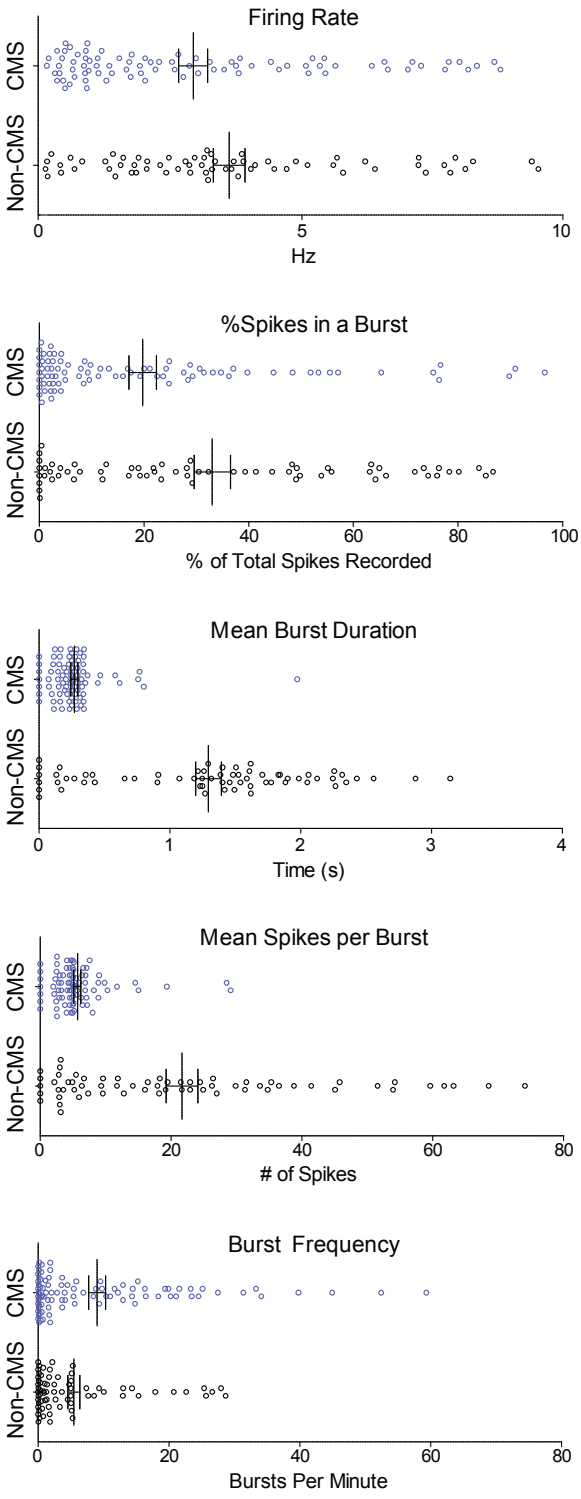

Supplementary Figure 8: Group differences in baseline VTA recordings are observed in animals that underwent CMS relative to non-stressed controls. Here, all cells with firing rates <10 Hz are plotted, for CMS (n=84) and non-CMS (n=66). Units recorded could represent DA or non-DA neurons in VTA. Statistics for all comparisons including cells firing at higher mean rates are detailed in Supplementary Figure 9.

Excluding cells with firing rates greater than 10 Hz										
Measure	**Firing Rate (Hz)**		**% Spikes in a Burst**		**Burst Duration (s)**		**Mean Spikes in a Burst**		**Bursts Per Minute**	
Group	Non-CMS	CMS	Non-CMS	CMS	Non-CMS	CMS	Non-CMS	CMS	Non-CMS	CMS
Number of values	66	84	66	84	66	84	66	84	66	84
25% Percentile	1.779	0.8536	6.289	2.196	0.5966	0.1587	5.14	3.203	0.2017	0.2664
Median	3.194	1.999	28.23	8.97	1.41	0.248	18.24	4.909	1.696	1.843
75% Percentile	5.232	4.684	57.69	29.18	1.853	0.314	34.91	6.575	5.269	12.07
Mean	**3.702**	**2.913**	**33.9**	**19.72**	**1.323**	**0.2697**	**24.08**	**5.672**	**5.199**	**6.597**
Std. Deviation	2.573	2.527	28.58	24.31	0.8243	0.2446	23.66	4.871	7.747	8.363
Std. Error	0.3167	0.2757	3.518	2.652	0.1015	0.02669	2.913	0.5314	0.9536	0.9124
Lower 95% CI	3.069	2.365	26.88	14.44	1.121	0.2166	18.26	4.615	3.295	4.782
Upper 95% CI	4.334	3.461	40.93	24.99	1.526	0.3228	29.89	6.729	7.104	8.412
Mann-Whitney U	**P value**	**0.0314**	**P value**	**0.0033**	**P value**	**< 0.0001**	**P value**	**< 0.0001**	**P value**	**0.4253**

Including all cells recorded										
Measure	**Firing Rate (Hz)**		**% Spikes in a Burst**		**Burst Duration (s)**		**Mean Spikes in a Burst**		**Bursts Per Minute**	
Group	Non-CMS	CMS	Non-CMS	CMS	Non-CMS	CMS	Non-CMS	CMS	Non-CMS	CMS
Number of values	71	93	71	93	71	93	71	93	71	93
25% Percentile	1.829	0.8681	6.77	2.311	0.7301	0.1628	5.463	3.431	0.3238	0.3771
Median	3.282	2.515	29.22	11.64	1.483	0.2516	19.48	5	1.778	3.574
75% Percentile	6.216	5.549	64.97	38.43	2.05	0.3397	38.8	7.358	5.273	14.4
Mean	**4.371**	**4.125**	**37.93**	**25.38**	**1.574**	**0.5958**	**36.46**	**12.51**	**5.427**	**8.991**
Std. Deviation	3.695	4.608	31.25	29.46	1.359	1.95	60.42	40.6	7.812	12.39
Std. Error	0.4385	0.4778	3.709	3.054	0.1612	0.2022	7.171	4.21	0.9271	1.285
Lower 95% CI	3.497	3.177	30.53	19.31	1.253	0.1942	22.15	4.151	3.578	6.439
Upper 95% CI	5.246	5.074	45.33	31.44	1.896	0.9974	50.76	20.87	7.276	11.54
Mann-Whitney U	**P value**	**0.1172**	**P value**	**0.0122**	**P value**	**< 0.0001**	**P value**	**< 0.0001**	**P value**	**0.1693**

Supplementary Figure 9: Statistics of firing properties in VTA recordings from CMS and non-CMS rats. Using a non-parametric Mann-Whitney U test, we compared Firing Rate (Hz), the proportion of total spikes recorded that were within a burst, mean burst duration (s), mean spikes per burst, and burst frequency. As above, units recorded could represent DA or non-DA neurons in VTA. Comparisons were computed for the entire data set (n=164 cells) and cells that had firing rates lower than 10 Hz (n=150 cells).

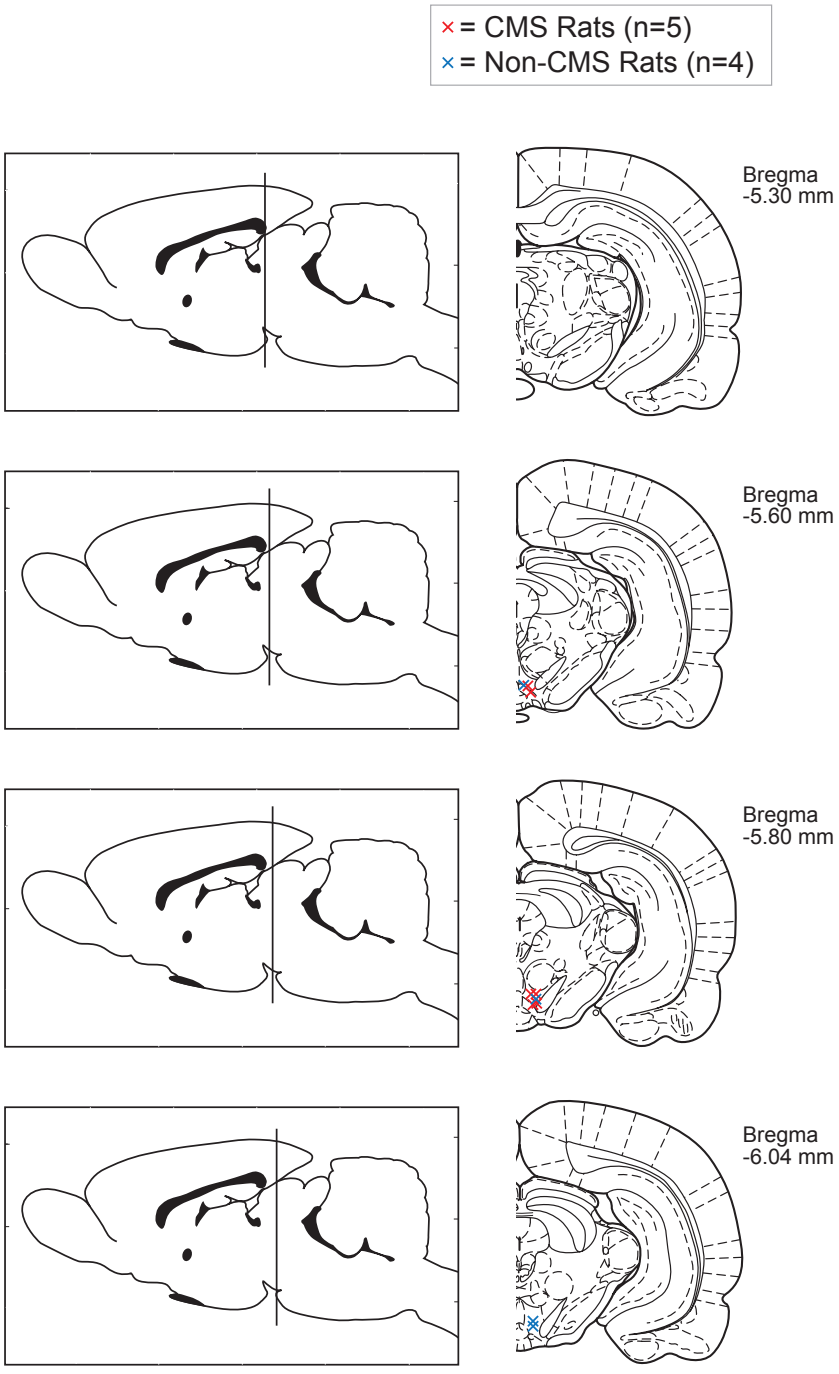

Supplementary Figure 10: Histologically verified electrode tips from VTA recordings in Supplementary Figures 8 and 9. Following recording sessions, electrolytic lesions were created for placement confirmation, as indicated by the crosses.

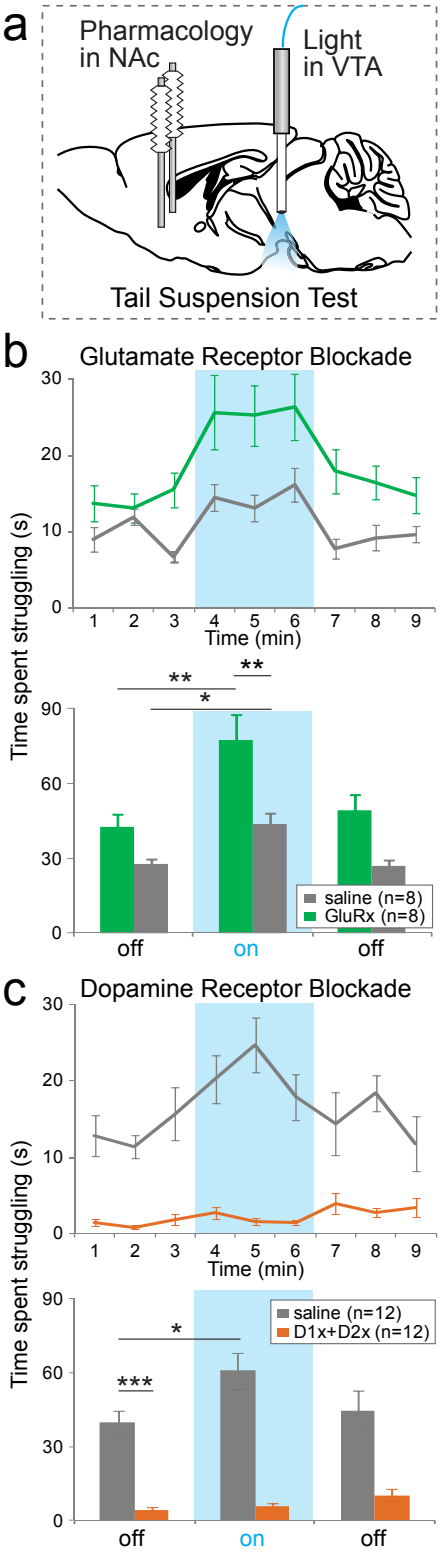

Supplementary Figure 11: Dopamine, but not glutamate, receptor signaling is required for mediating escape-related behavior. To determine whether NAc glutamate or dopamine receptor signaling was critical for mediating the light-induced

changes in escape related behavior, we combined pharmacological and optogenetic techniques. **a**, Schematic representation of bilateral NAc pharmacological manipulation in combination with VTA-DA neuron illumination in animals treated with CMS. **b**, Antagonism of glutamate receptors (GluRx) in the NAc does not block the baseline levels of struggling nor the light-induced increase in escape-related behavior on the tail suspension test. We performed within-subject comparisons counter-balanced for order, and infused either saline, or a mixture of the α-amino-3-hydroxy-5-methyl-4-isoxazolepropionic acid receptor (AMPAR) antagonist 2,3-dihydroxy-6-nitro-7-sulfamoyl-benzo[f]quinoxaline-2,3-dione (NBQX) and the N-Methyl-D-aspartate receptor (NMDAR) antagonist (2R)-amino-5-phosphonovaleric acid (AP5), into the NAc just prior to the TST. Following intra-NAc saline treatment, we replicated the rescue of the stress-induced depression-like phenotype upon VTA illumination (1-way ANOVA, $p<0.001$, Dunn post-hoc test comparing baseline to light-on epochs, $^{*}p<0.01$). Following intra-NAc glutamate receptor blockade, rescue of the stress-induced depression-like phenotype upon illumination was not blocked (1-way ANOVA, $^{**}p<0.001$, Dunn post-hoc test comparing baseline to light-on epochs, $^{**}p<0.001$). Indeed, the amount of time spent struggling was greater overall in the animals treated with glutamate receptor antagonists; 2-way ANOVA revealed a significant group-by-light epoch interaction ($F_{2,28}=3.69$, $p=0.0379$), a significant effect of experimental group ($F_{1,14}=7.24$, $p=0.0176$), and a significant effect of light epoch ($F_{2,28}=38.98$, $p<0.0001$). Since the NAc receives robust glutamatergic innervation from a number of regions, including the PFC, amygdala and hippocampus, we speculate that the net effect of these inputs may serve to suppress escape-related behavior on the TST; these findings may be consistent with recent studies showing that ketamine, an NMDAR antagonist, can acutely improve depression symptoms in humans[2–4]. **c**, Antagonism of D1 and D2 dopamine receptors (D1x+D2x) in the NAc attenuates escape-related behavior. Since glutamate transmission in the NAc was not required for mediating the light-induced increase in escape-related behavior during TST, we next tested whether DA signaling in the NAc could be critically involved in modulating the escape-related behavior. We again performed a within-subjects comparison, now following intra-NAc saline or intra-NAc DA receptor antagonism, using a cocktail of SCH23390 (D1 receptor antagonist) and raclopride (D2 receptor antagonist) prior to testing on the TST. We observed a significant attenuation of escape-related behavior with NAc DA receptor blockade during both baseline and illumination epochs (2-way ANOVA revealed a significant drug-by-light epoch interaction, $F_{2,44}=3.52$, $p=0.0381$, a significant effect of drug, $F_{1,22}=53.74$, $^{***}p<0.0001$, and a significant effect of light epoch, $F_{2,44}=3.48$, $p=0.0395$).

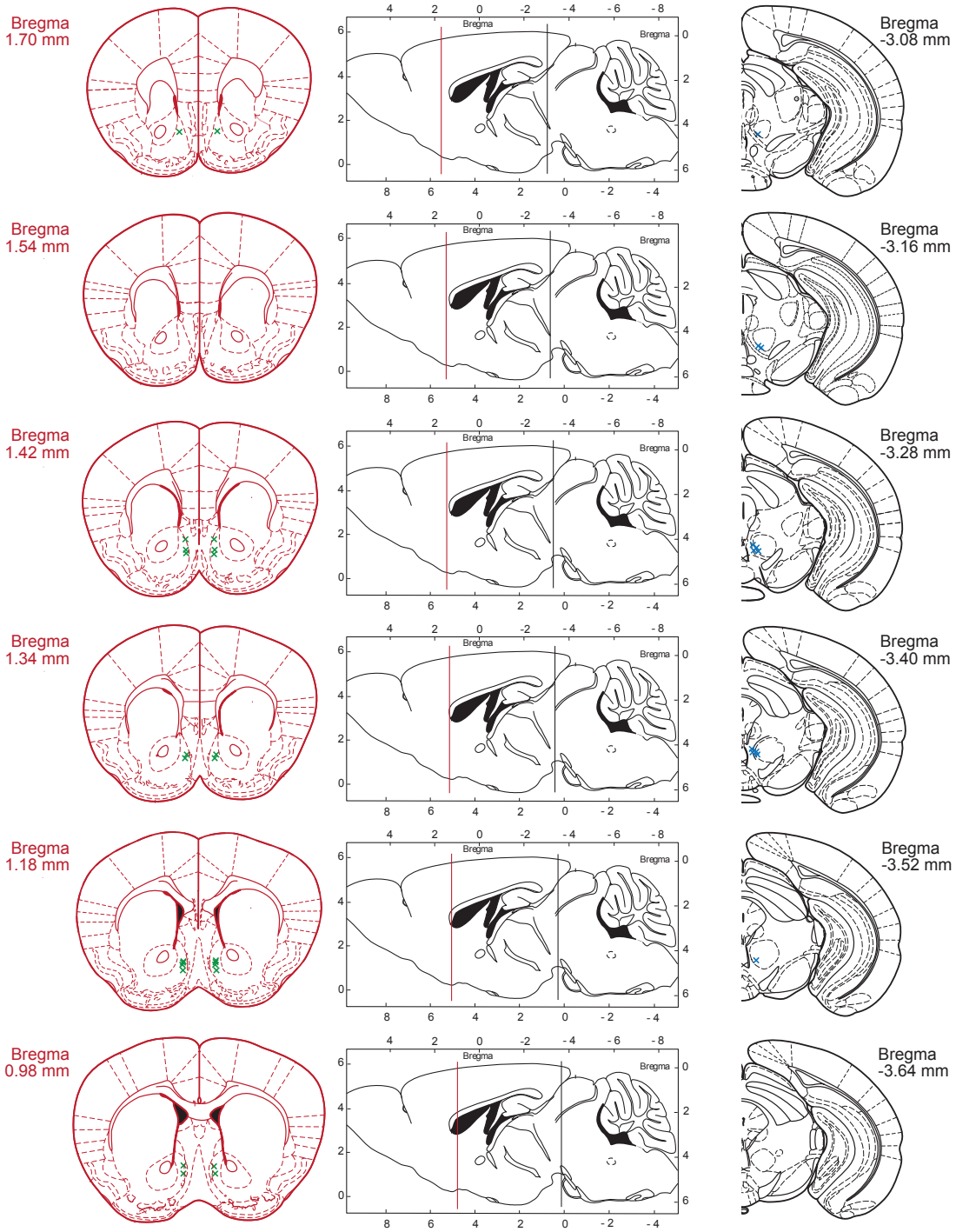

Supplementary Figure 12: Histological verification for all animals included in Supplementary Fig. 11, exposed to pharmacology in the NAc and optogenetic manipulation of VTA-DA neurons. For each sagittal diagram (center column), the red line refers to the red diagrams (cannula placement in Nac), and the black line refers to the black diagrams (fiberoptic placement in VTA). Cannula infusion tip placements are indicated with green symbols and optical fiber tips are indicated with blue symbols on the corresponding diagrams.

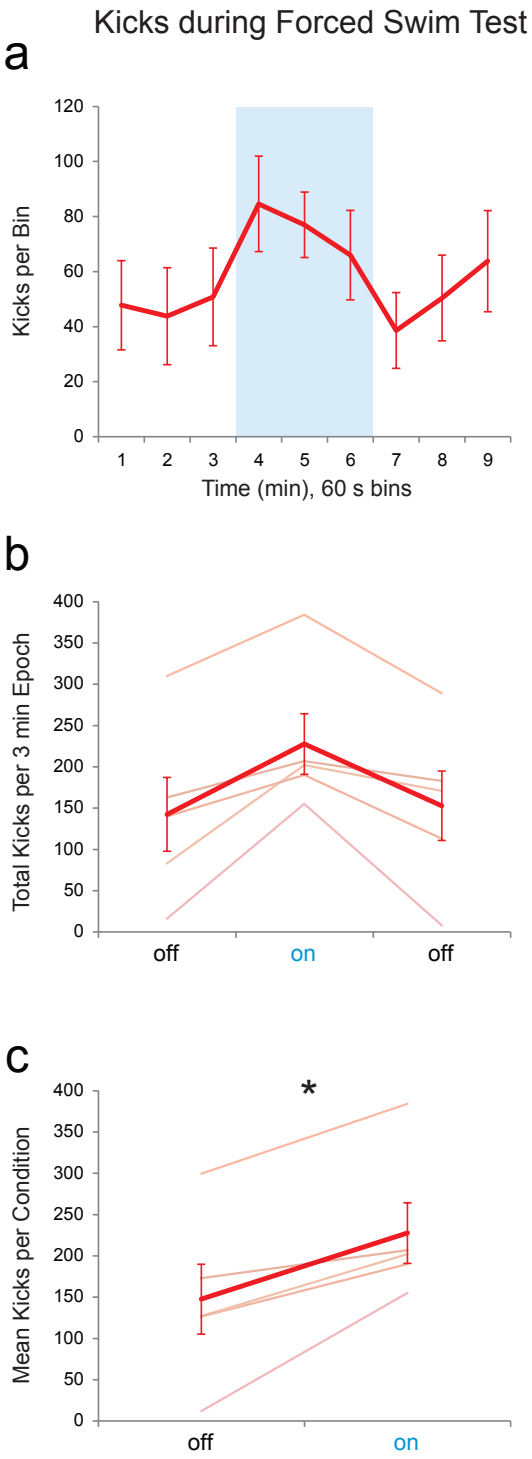

Supplementary Figure 13: Analysis of first light-on epoch in TH::Cre rats during FST. Here, to ensure that we were not biasing our comparison of single-epoch OFT and multiple epoch FST behavioral analyses, we performed statistical analysis of only the 9-min surrounding the first light-on epoch in the FST. We observed a significant effect of light on kicking activity in a Paired t-test, *p=0.0110.

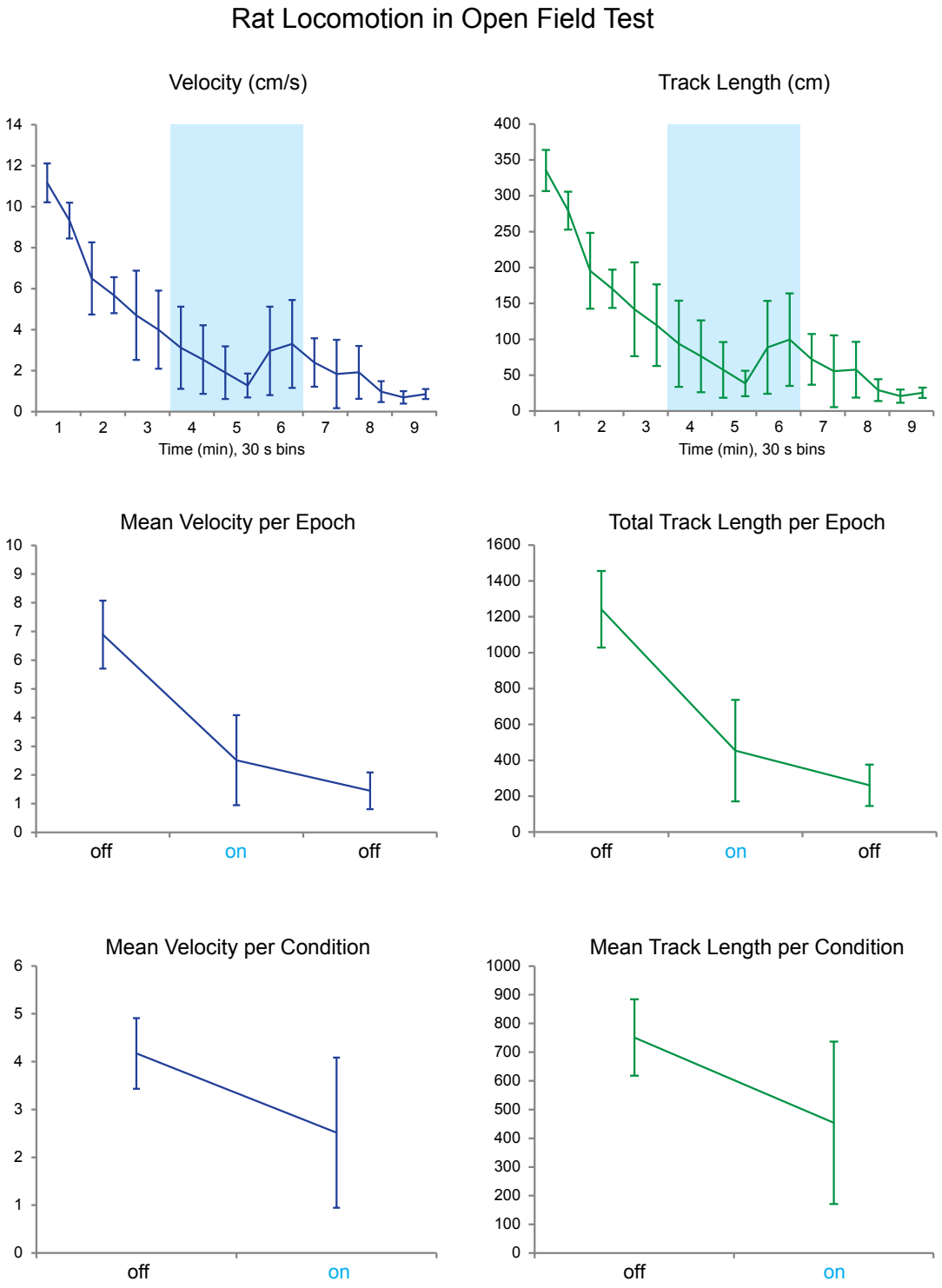

Supplementary Figure 14: Additional analysis of TH::Cre rat locomotion in OFT. Using the same epoch duration of 9-min, with 3-min epochs in the OFT, we did not observe significant effects of illumination on locomotion, neither as measured by velocity nor track length (Paired t-test, p=0.1683 and p=0.1688, respectively). As noted above, modest effects if present and significant would still be consistent with clinical observations[1].

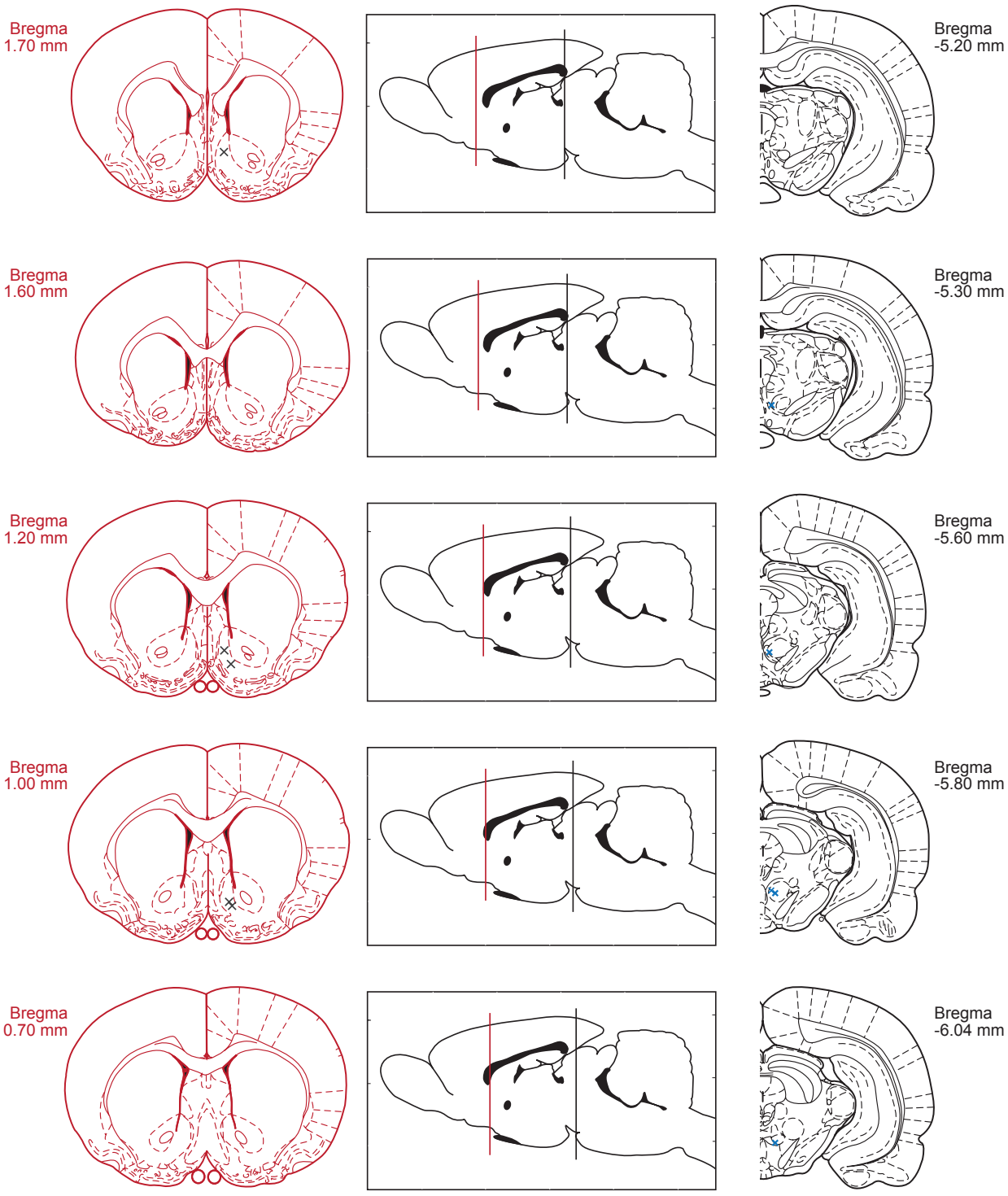

Supplementary Figure 15: Histological verification for all animals included in Fig. 4, Supplementary Figure 13 and 14. Electrode array tip placement is shown for the nucleus accumbens medial shell (left), and optical fiber tip placement is shown above the ventral tegmental area (gray, n=5). Viral expression at the site of the fiber tip was also confirmed (not shown). Gray symbols in left column indicate the center of the electrolytic lesion created just prior to sacrifice to identify the location of the electrode array tips. Blue symbols in right column indicate tip of the fiber.

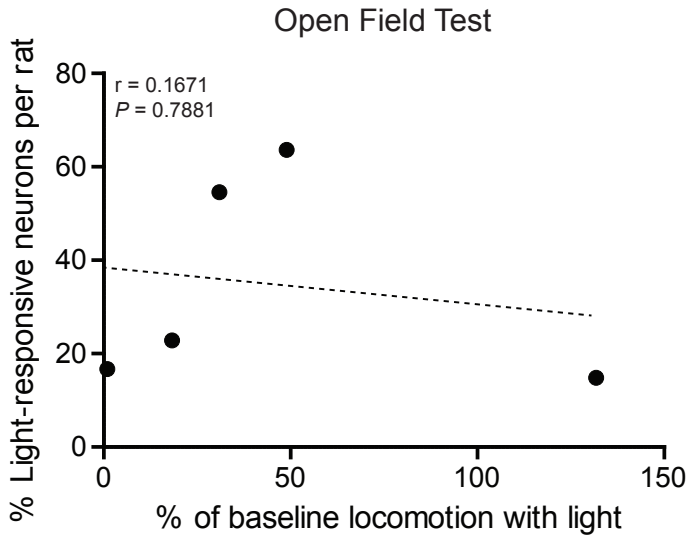

Supplementary Figure 16: Linear regression of the proportion of light-responsive neurons in the NAc and locomotor activity in the OFT. There was no significant correlation between the proportion of neurons that showed phasic responses to light trains in the VTA and locomotion in the open field (Pearson's Correlation Test, p=0.7881).

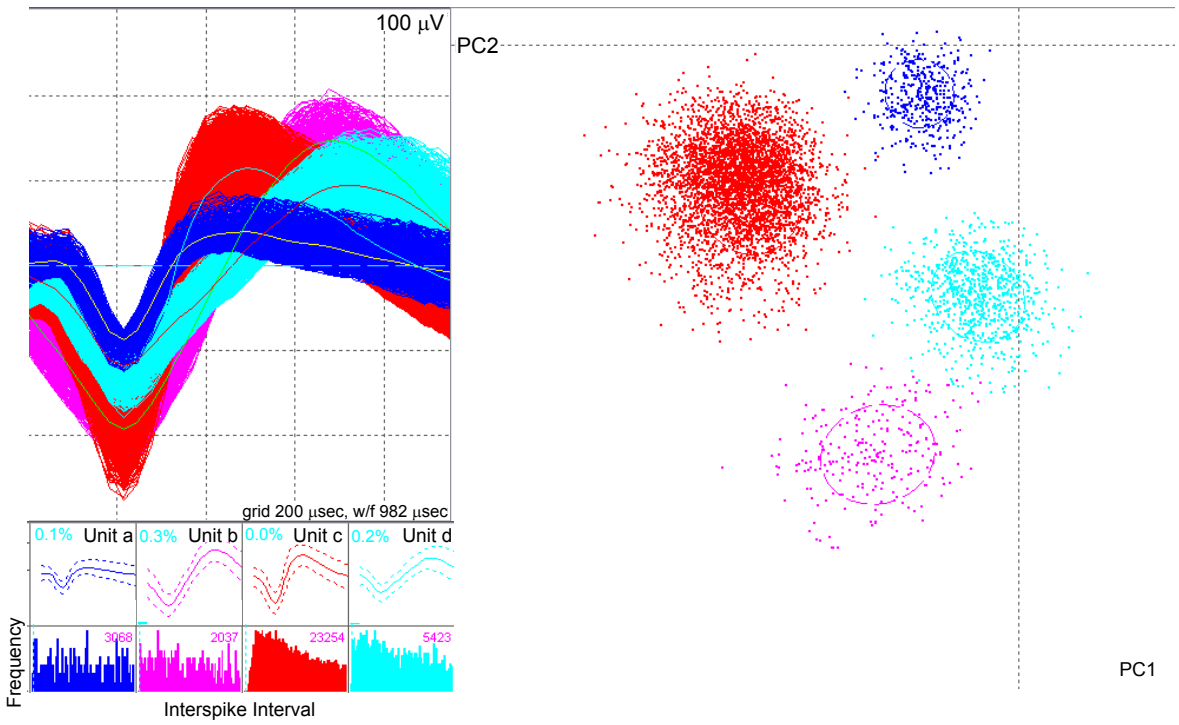

Supplementary Figure 17: Representative single-unit recording approach shown for 4 NAc units. At upper left, the 4 example waveforms (w/f) are shown with corresponding inter-spike interval (ISI) histograms below. The ISI histograms span 0 to 100 ms in 1 ms bins, where the y-axis represents the frequency of spikes occurring at each ISI, and the magenta number indicates the number of waveforms collected per identified unit. The blue number indicates the proportion of spikes that show an ISI below threshold, indicated by the vertical blue dotted lines (here threshold is 1500 μsec). At right, these same neurons are shown in the principal-component analysis clustering display.

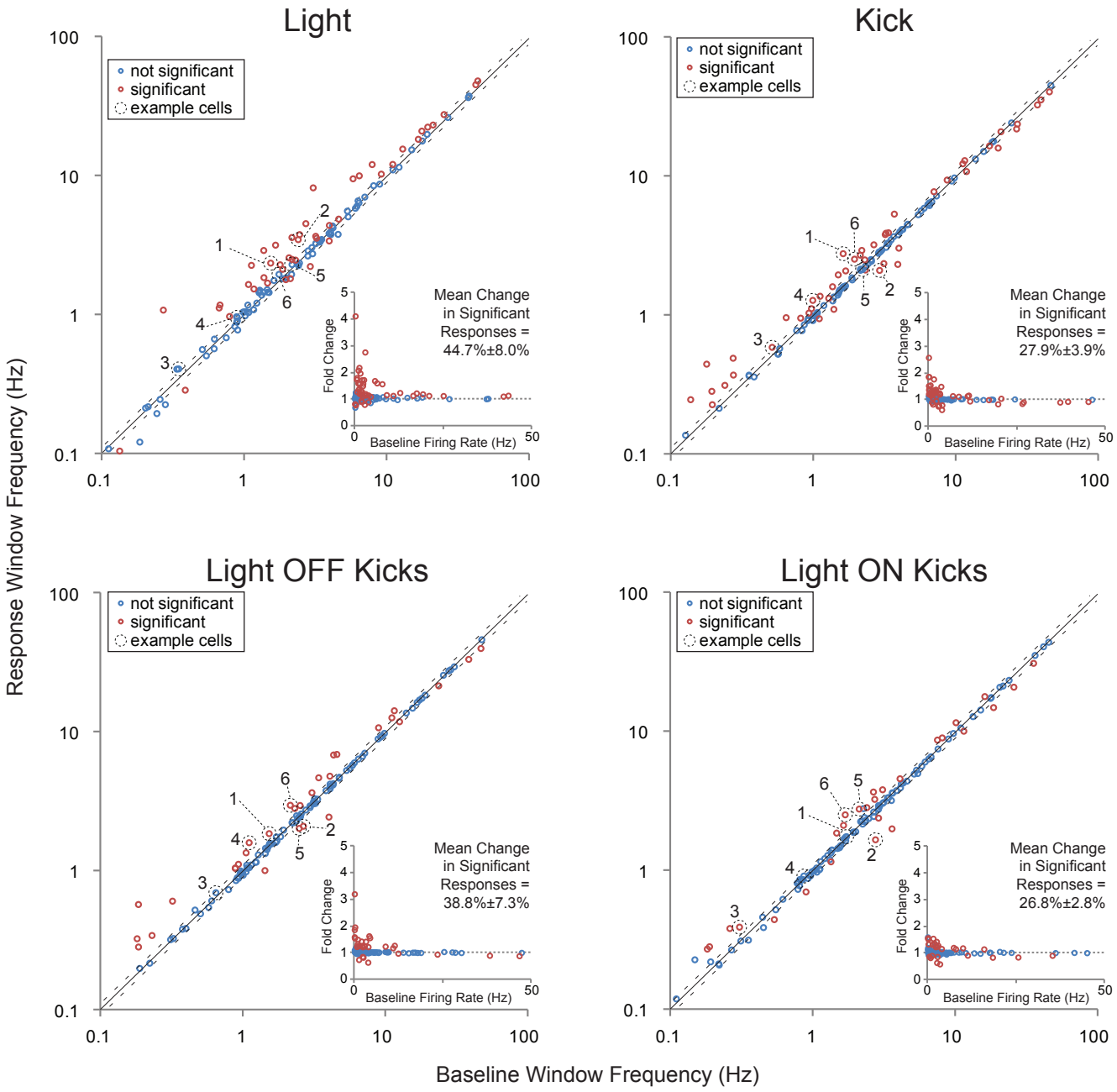

Supplementary Figure 18: NAc firing rate changes observed during optical stimulation and escape behavior. Scatter plots show firing rate during the response window for a reference event (Light, Kick, Light OFF Kicks, Light ON Kicks) plotted on a log-log scale against firing rate within a baseline window (see methods) for all 123 neurons recorded within NAc. The solid diagonal line indicates values for which the firing rates in these two windows were identical; dashed black lines indicate ± 10% change in firing rate. Blue circles indicate cells that tested not significant ($p \geq 0.05$; methods); Red circles indicate cells that showed a significant change in firing rate between the baseline and response windows ($p<0.05$). The fractional change in the

average firing rate between the baseline and response window was computed across all event occurrences, and the significance of this change was determined by its percentile position within a bootstrap distribution estimated using 500 random circular permutations of spike times relative to events times. The cells demarcated with a dotted circle are the Fig. 4 example cells; each number corresponds to the cell number used in Fig. 4. The insets of each graph show the fold change (4 fold reflects a 300% increase) in firing rate for each reference event plotted against each cell's baseline firing rate.

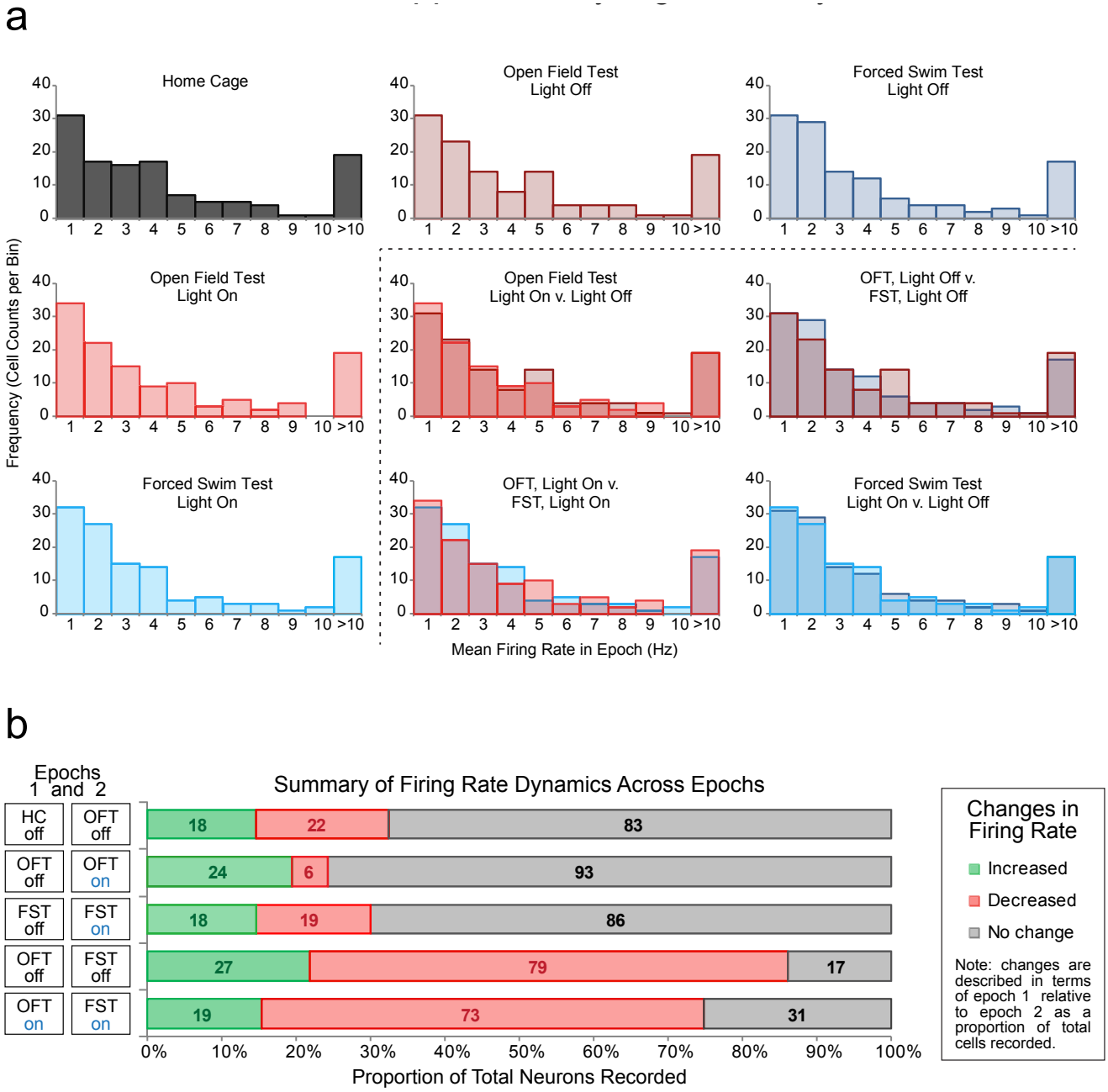

Supplementary Figure 19: Population summaries of firing rate dynamics within each epoch. Mean firing rate change relative to baseline in significant responses for each reference event was as follows: Light = 44.7%±8.0%; Kick = 27.9%±3.9%; Light off kicks = 38.8%±7.3%; Light on kicks = 26.8%±2.8%. **a**, Histograms below and to the right of the dotted line allow for direct comparisons of the distribution of neurons during epoch, as the histograms are overlaid. **b**, Summary of overall changes in firing rate depicted below reveal that discrete populations of neurons show distinct firing rate dynamics in opposing directions, which may reduce the observable change when only comparing population distributions as a whole rather than individual neuron changes.

Supplementary References

1. Lemke, M. R., Wendorff, T., Mieth, B., Buhl, K. & Linnemann, M. Spatiotemporal gait patterns during over ground locomotion in major depression compared with healthy controls. *Journal of Psychiatric Research* **34**, 277–283 (2000).
2. Berman, R. M. *et al.* Antidepressant effects of ketamine in depressed patients. *Biological Psychiatry* **47**, 351–354 (2000).
3. Maeng, S. *et al.* Cellular Mechanisms Underlying the Antidepressant Effects of Ketamine: Role of α-Amino-3-Hydroxy-5-Methylisoxazole-4-Propionic Acid Receptors. *Biological Psychiatry* **63**, 349–352 (2008).
4. Zarate, C. A. *et al.* A Randomized Trial of an N-methyl-D-aspartate Antagonist in Treatment-Resistant Major Depression. *Arch Gen Psychiatry* **63**, 856–864 (2006).
5. Tsai, H.-C. *et al.* Phasic Firing in Dopaminergic Neurons Is Sufficient for Behavioral Conditioning. *Science* **324**, 1080 –1084 (2009).